

**MONITORING OF SOLAR SYSTEMS -  
THEORETICAL AND EXPERIMENTAL INVESTIGATION  
ON MEASUREMENTS OF SOLAR RADIATION**

**M. Uecker, M. Krause, K. Vajen, H. Ackermann**

FB Physik, Universität Marburg, Renthof 5, 35032 Marburg, Germany,  
Ph. ++49-(0)6421/282-4131, Fax /282-6535, solar@physik.uni-marburg.de

**Abstract** – The incoming radiation or more exactly the radiation being absorbed by a collector, is one of the most influential factors on the solar yield of a solar thermal system. Hence, a powerful monitoring especially of large solar thermal systems would not work without measuring the radiation with (at least) one (usually additional) sensor. Uncertainties due to the radiation occur, when the absorbed radiation has to be estimated. They depend on the accuracy of the used solar sensor, the plane, in which the sensor has been installed, the diffuse correlation and conversion models used for the estimation of the radiation-distribution over the sky and the incidence angle corrections for the used collector. Experimental comparisons yield, that properly calibrated PV-cells achieve acceptable accuracy for monitoring solar systems. The installation of the used sensor in collector plane instead of in horizontal plane should be preferred since it allows to determine the absorbed radiation with a lower uncertainty due to the estimation of the different fractions of the global radiation. For the estimation of the different fractions of the global radiation, the combination of the diffuse correlation method from Erbs together with the conversion model from Hay-Davies represents the measured data in a best way. More detailed methods do not provide better results in the scope of the investigated data. Additionally it could be shown that the consideration of the incidence angle correction has to be done with care, since typically used approximations could lead to not negligible deviations.

## 1. INTRODUCTION

The practical experiences from the construction and operation of solar thermal systems show that failures or operation bugs occur, which are often not detected (not even by experienced service staff). For this reason a powerful monitoring of solar systems seems to be necessary to achieve the expected solar yields and fossil fuel savings. Here we confine our investigations to system monitorings, which compare (e.g. on a daily time resolution) the measured solar yield with calculated values by a system model. Typically, the incoming radiation is the most influential factor on the solar yield of a solar thermal system (see fig.1). Hence, a powerful monitoring especially of large solar systems would not work without measuring and considering the solar radiation.

An important problem in connection with the consideration of radiation is to ask in fig.1, if a variation of  $Q_{sol}$  for constant  $H^T$  belongs to the remaining uncertainty due to the solar radiation influence, to other influential factors (e.g. water consumption, ambient temperature) or if it indicates a poor system performance. In this paper we are interested in the remaining deviation due to the solar radiation influence.

For considering the solar radiation, there is a need for (at least) one solar sensor, which might be not installed anyway at a solar thermal system. Due to this it is necessary to accept a compromise between the costs and the accuracy of this sensor. Besides this it must be kept in mind that the quantity, which

characterizes the influence of the incoming radiation on the solar gain in the most suitable way, is the radiation absorbed by the absorber,  $G_{use}$ , and not the global irradiance in the collector plane.  $G_{use}$  depends on the distribution of the radiation incident on the collector  $G(J, j)$ , the transmission-absorption-product for vertical incidence and the incidence-angle-modifier (IAM( $J, j$ )). It can be calculated by

$$G_{use} = \iint_{J, j} \tau a(q) G(J, j) \cos q \sin J \, dJ \, dj$$

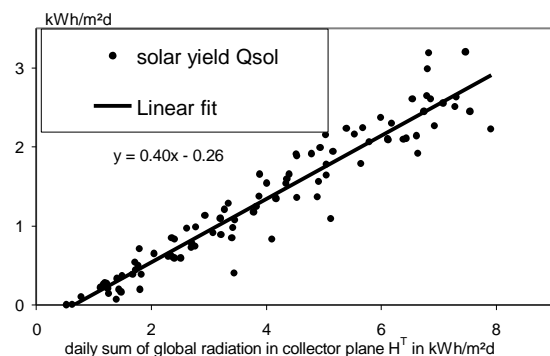


**Fig. 1 Input-Output-Diagram for the solar thermal system in Zwickau (cf. fig.10) for the period 1.7-30.9.98.  $Q_{sol}$  is the daily solar yield measured at the secondary side of the heat exchanger between collector and solar storage and is (as shown) strongly correlated with the daily sum of the global radiation  $H^T$  in the collector plane. The deviation from perfect correlation is caused by the remaining influence of the solar radiation, by other influential factors (e.g. heat demand) or indicates a poor system performance.**

The equation shows that when calculating  $G_{use}$ , one needs to determine the distribution of the radiation  $G(\mathbf{J}, \mathbf{j})$  in dependence on the measurand of the sensor (e.g.  $G^H$ ,  $G^T$ ). There are several approaches to do this determination (see section 2 and 3), however they require the global horizontal radiation  $G^H$  as input. This entails the disadvantage that the global radiation in collector plane  $G^T$  is already uncertain due to model errors. We refined these methods to apply them also for data measured in the collector plane but along this refinement new uncertainties occur (see section 4).

Regarding these facts the following questions arise when asking which way would be the best to consider the radiation when monitoring solar systems:

- Which algorithm should be used to estimate  $G(\mathbf{J}, \mathbf{j})$  ?
- In which plane should be measured (horizontal or collector) ?
- Which influence has the method of the incidence angle modifier correction ?
- Which accuracy should have the radiation sensor ?
- What are the remaining uncertainties due to the influential factor "solar radiation" ?

To answer these questions the following investigations were carried out on the basis of two data sets, measured at large solar thermal systems (data basis: 1/2-hr mean values of  $G^H$  and  $G^T$  measured with CM11-pyranometers, locations: Leipzig/Zwickau (both Germany), data period: 1 year/ 1 year, azimuth of the collector fields: south  $\pm 10^\circ$ , slope of the collectors:  $30^\circ/45^\circ$ ):

- Comparison of the  $G^T$  values calculated from  $G^H$  and measured values of  $G^T$  to estimate the quality of the models to determine the solar radiation distribution  $G(\mathbf{J}, \mathbf{j})$  (section 2).
- Calculation of  $G_{use}$  from the measurands  $G^T$  and  $G^H$  for different models which estimate the solar radiation distribution. Since  $G_{use}$  is not a measurand (or really difficult to measure), the variation of  $G_{use}$  due to different radiation distribution determination models was taken to decide in which plane should be measured. (section 3 and 4).
- Comparison of the useful radiation  $G_{use}$  calculated from the measurand  $G^T$  and  $G^H$  for different detailed approximations of the incidence angle correction methods to quantify the approximation error (section 5).
- Relating to the influence of the accuracy of the radiation sensor, simultaneous measurements of different solar sensors have been carried out to estimate the deviations of these sensors referring to a CM 11 pyranometer. On this basis the influence of the sensor accuracy on the determination of  $G_{use}$  has been investigated (section 6).

Since the results are systematically very similar for both, Leipzig and Zwickau data, only the results on the basis of the Zwickau data are shown here.

The influence of solar radiation and especially of  $G_{use}$  on the solar yield  $Q_{sol}$  depends on the system concept and other boundary conditions (e.g. consumption, ambient temperatures, storage temperatures). To get an impression of the possible uncertainties of  $Q_{sol}$  for large solar thermal systems with a typical German system concept, we carried out several TRNSYS-simulations of two systems which have been measured in Leipzig and Zwickau ( $A_{Coll}=398/158 \text{ m}^2$ ,  $V_{Storage}=20/9 \text{ m}^3$ ,  $Q_{load}/\text{day}=5-20/1-11 \text{ kWh/m}^2\text{d}$ .) (section 7).

Against the background of monitoring systems, the uncertainties of  $H^T$ ,  $H_{use}$  and  $Q_{sol}$  due to the consideration of solar radiation which will be presented in the next sections have to be compared with the accuracy of system model results for the solar yield. To give an idea of the latter accuracy, the calculation results for the solar yield of a very simple and a very detailed system model are compared with the measured values in fig. 2 for the system in Zwickau. The Input-Output-Function derived as the linear fit of the presented data in fig.1 is used as a simple model. The detailed model is a variant of the TRNSYS-model described in section 7. For the comparison of measured and calculated values the solar yield is determined at the heat exchanger between collector and storage ( $Q_{sol}$ ) as well as at the heat exchanger for discharging the solar buffer store ( $Q_{sol2}$ ). The detailed model achieves an accuracy of  $\pm 0.1 \text{ kWh/m}^2\text{d}$  for both values  $Q_{sol}$  and  $Q_{sol2}$ . As opposed to that, the simple Input-Output-model, which only considers  $G_T$  and no other influential factors, achieves in the case of  $Q_{sol}$  an accuracy of circa  $\pm 0.4 \text{ kWh/m}^2\text{d}$ . Since a part of  $Q_{sol}$  is sometimes stored in the solar storage till the next day, the accuracy diminished for the Input-Output-model to  $\pm 0.75 \text{ kWh/m}^2\text{d}$ , (see  $Q_{sol2}$ ). This storage process is obviously well modeled in the detailed TRNSYS model.

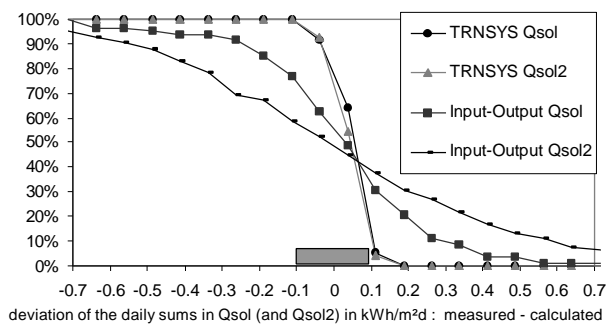


**Fig. 2** Relative summarized frequency of the deviation between measured and calculated daily solar yield  $Q_{sol}$  and  $Q_{sol2}$  of the system in Zwickau (cf. fig. 10) for a simple (Input-Output) and a detailed system model (TRNSYS).  $Q_{sol2}$  is the daily solar yield measured at the primary side of the heat exchanger for discharging the solar storage (data for period 1.7.-30.9.98). The simple model in the case of  $Q_{sol}$  is the Input-Output-Function derived from fig. 1. In the case of  $Q_{sol2}$  a second Input-Output-Function is derived from n diagram analogous to fig.1. The detailed model is a variant of the TRNSYS model described in section 7. For the results presented in fig.2 the TRNSYS-model uses both  $G_T$  and  $G_H$  as measurand inputs.

## 2. CALCULATION OF SOLAR RADIATION ON A TILTED SURFACE

In the literature many methods are described to determine the global radiation on a tilted surface  $G^T$  from hourly values of the global horizontal radiation  $G^H$ . To simplify the determination, the whole distribution of solar radiation has to be divided into a fraction coming directly from the sun  $G_{\text{Beam}}^T$ , a fraction coming reflected isotropic from the ground  $G_{\text{Ground}}^T$ , a fraction coming isotropic from the sky  $G_{\text{Diffuse}}^{\text{iso},T}$ , a fraction coming from the circumsolar region  $G_{\text{Diffuse}}^{\text{C},T}$  and a fraction coming from the horizon  $G_{\text{Diffuse}}^{\text{Hor},T}$ . Hereby,  $G^T$  can be calculated by (1).

$$\begin{aligned} G^T &= G_{\text{Beam}}^T + G_{\text{Ground}}^T + G_{\text{Diffuse}}^{\text{iso},T} + G_{\text{Diffuse}}^{\text{C},T} + G_{\text{Diffuse}}^{\text{Hor},T} = \\ &= G^H (1 - k_d) \frac{\cos(\mathbf{q})}{\cos(\mathbf{J}_z)} + G^H \Gamma_{\text{Ground}} \frac{1 - \cos(\mathbf{b})}{2} + \\ &G^H (1 - k_d) \left( \frac{\cos(\mathbf{q})}{\cos(\mathbf{J}_z)} F^C + \frac{1 + \cos(\mathbf{b})}{2} (1 - F^C) + \sin(\mathbf{b}) F^{\text{Hor}} \right) \end{aligned} \quad (1)$$

The different methods, which have been taken into account in this presentation, differ in the estimation of the diffuse fraction  $k_d = G_{\text{Diffus}}^H / G^H$  (Liu and Jordan 1960, Boehs et al. 1976, Erbs et al. 1982, Reindl et al. 1990) as well as in the following determination of the different portions of the diffuse radiation ("isotropic", (Hay and Davies 1980, Reindl2 et al. 1990, Perez et al. 1988)) i.e in the choice of  $F^C$  and  $F^{\text{Hor}}$ . Instead of the determination of the diffuse portions, the determination of  $G_{\text{Beam}}^T$  and  $G_{\text{Ground}}^T$  is done in all calculations in the same way.

For the estimation of  $k_d$ , many correlation models have been developed. The most important correlation depends on the clearness index  $k_t = G^H / I^{\text{Ext}}$ , more detailed models additionally on the zenith angle  $\mathbf{J}_z$ . As measured values show, the determination of  $k_d$  as a function of  $k_t$  has great uncertainties, which are up to  $\pm 25\%$ -points. Due to this, two further methods have been implemented to estimate the maximum and minimum deviations of  $G^T$  (resp.  $G_{\text{use}}(G^H)$ , cf. (7)), causing from the  $k_d$ -uncertainty. In these versions (Erbs-Max, Erbs-Min) the maximum and minimum values of  $G^T$  (resp.  $G_{\text{use}}(G^H)$ ) are taken into account, which result from the  $\pm 25\%$ -points variation of the diffuse fraction, calculated by the Erbs-correlation:

$$\begin{aligned} G_{\text{Erbs-Max}}^T &= \\ &\text{Max} \left( G^T \left( \text{Min}(1, k_d^{\text{Erbs}} + 0.25) \right), G^T \left( \text{Max}(0.1, k_d^{\text{Erbs}} - 0.25) \right) \right) \\ G_{\text{Erbs-Min}}^T &= \\ &\text{Min} \left( G^T \left( \text{Min}(1, k_d^{\text{Erbs}} + 0.25) \right), G^T \left( \text{Max}(0.1, k_d^{\text{Erbs}} - 0.25) \right) \right) \end{aligned}$$

To decide, which combination of the diffuse fraction and conversion models should be used for the estimation of the

global radiation on a tilted surface, the calculated radiation on this surface was compared with the measured. The results presented in fig. 3 show, that the lowest deviation from the measured values achieves the combination Erbs/Hay-Davies.

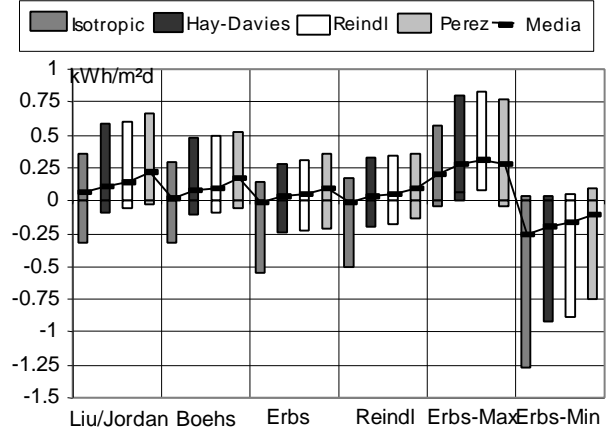


**Fig. 3: Influence of the combination of diffuse correlation and conversion models on the calculated daily sum  $H^T$  of  $H^T(G^{\text{H,meas}})$ , represented as the deviation from  $H^{\text{T,meas}}$ :  $DH^T = H^T(G^{\text{H,meas}}) - H^{\text{T,meas}}$ . Represented in the figure is the median of the deviations of the daily sums for each variant and the interval, in which 90% of the deviations are included.**

The best estimation of the global radiation on a tilted surface succeeds with the combination Erbs/Hay-Davies. However, the deviations  $DH^T$  are (very) high. The annual sum differs between 0 and 100 kWh/m<sup>2</sup>a. The good performances of the combinations Liu-Jordan/Isotropic and Boehs/Isotropic indicate that Liu-Jordan and Boehs seem to be suitable to estimate  $k_d$  excluding the circumsolar diffuse fraction. The more detailed conversion models Reindl and Perez and also the more detailed diffuse correlation of Reindl do not lead to better results than the combination Erbs/Hay-Davies within the scope of the investigated data.

## 3. DETERMINATION OF THE USEFUL RADIATION

To calculate the energy absorbed by a flat plate collector, a correction accounting for the different incident angles has to be done. This correction is necessary due to the angular dependence of the transmission and absorption of the collector glass plate, the absorption of the absorber and the shading by the collector frame.

For calculating the absorbed energy the correction of the radiation incidence in the angles  $\mathbf{J}, \mathbf{j}$  can be described by the product of the transmission-absorption product for vertical incidence  $(\mathbf{ta})_{\perp}$  and the incidence angle modifier  $\text{IAM}(\mathbf{J}, \mathbf{j})$  (cf. (2)).

$$\mathbf{ta}(\mathbf{J}, \mathbf{j}) = (\mathbf{ta})_{\perp} \cdot \text{IAM}(\mathbf{J}, \mathbf{j}) \quad (2)$$

For flat plate collectors and by additionally neglecting anisotropic effects, the IAM-function only depends on the incidence angle on the surface  $\text{IAM}(\mathbf{q})$ .

For a collector one is interested in,  $\mathbf{ta}(\mathbf{q})$  has to be determined either with physical models (e.g. Fresnel-formulas to model transmission through the glazing) or in collector tests. In the latter case, the incidence angle modifier can be described by a

semiempiric formula, for example equation 3 (cf. Ambrosetti and Keller 1985):

$$IAM(\mathbf{q}) = 1 - \tan^{1/r}(\mathbf{q}/2) \quad (3)$$

Then, the useful radiation is given by:

$$G_{use} = \iint_{J,j} \mathbf{t}(\mathbf{q}) G(\mathbf{J}, \mathbf{j}) \cos(\mathbf{q}) \sin(\mathbf{J}) d\mathbf{J} d\mathbf{j} \quad (4)$$

The relationship between the different angles is given by:

$$\cos(\mathbf{q}) = \sin(\mathbf{J}) \cdot \sin(\mathbf{j}) \quad (5)$$

Since the exact distribution of the radiation over the sky is difficult to estimate, the global radiation is divided into the different diffuse and direct fractions as described in chapter 2, cf. (6).

$$G(\mathbf{J}, \mathbf{j}) = G_{Beam}(\mathbf{J}, \mathbf{j}) + G_{Ground}(\mathbf{J}, \mathbf{j}) + G_{Diffuse}^{iso}(\mathbf{J}, \mathbf{j}) + G_{Diffuse}^C(\mathbf{J}, \mathbf{j}) + G_{Diffuse}^{Hor,T}(\mathbf{J}, \mathbf{j}) \quad (6)$$

A correction factor is introduced for every fraction to consider the incidence angle dependence, which leads to the expression of  $G_{use}$ :

$$G_{use} = (\mathbf{t}(\mathbf{a}))_{\perp} \cdot \begin{pmatrix} K_{Beam} G_{Beam}^T + K_{Ground} G_{Ground}^T + \\ K_{Diffuse}^{iso} G_{Diffuse}^{iso,T} + K_{Diffuse}^C G_{Diffuse}^{C,T} + \\ K_{Diffuse}^{Hor} G_{Diffuse}^{Hor,T} \end{pmatrix} \quad (7)$$

To estimate the correction factors for the direct and the diffuse circumsolar radiation, the typical procedure is the assumption:

$$K_{Beam} = K_{Diffuse}^C = IAM(\mathbf{q}) \quad (8)$$

Since the aperture angle of the solar disc seen from earth is only  $0.5^\circ$ , this assumption is not very critical in the case of  $K_{Beam}$ . In the case of  $K_{Diffuse}^C$ , the circumsolar aperture angle varies and could reach values of  $40^\circ$ - $50^\circ$ . Due to this, the assumption is more critical especially for higher incidence angles and if the sun is just behind the collector. Since the aperture angle of the circumsolar radiation changes with the radiation situation, this effect has no simple dependence. This effect is discussed more detailed in (Uecker 2000) and is neglected here.

The distribution of the ground reflected radiation is normally assumed to be isotropic (c.f. Ineichen et al. 1990). For the estimation of  $K_{Diffuse}^{iso}$  and  $K_{Ground}$ , (Brandemuehl and Beckmann 1980) suggest an effective incidence angle  $\mathbf{q}_{Diffuse,eff}^{iso}$  respectively  $\mathbf{q}_{Ground,eff}$  depending on the collector slope. With these angles, the remaining correction factors are (variant Brandemuehl):

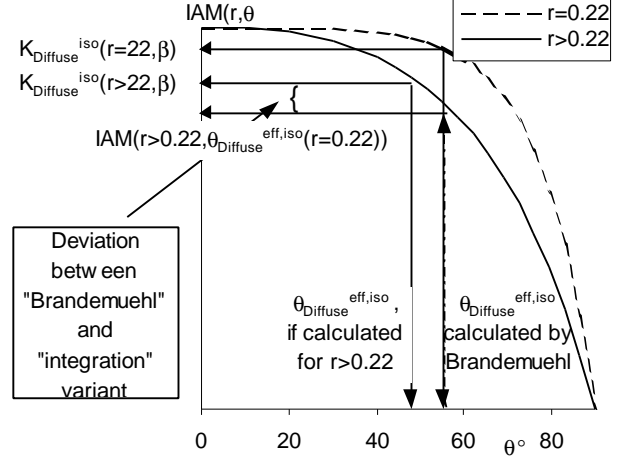
$$K_{Diffuse}^{iso} = IAM(\mathbf{q}_{Diffuse,eff}^{iso}) \quad (9)$$

$$K_{Ground} = IAM(\mathbf{q}_{Ground,eff}) \quad (10)$$

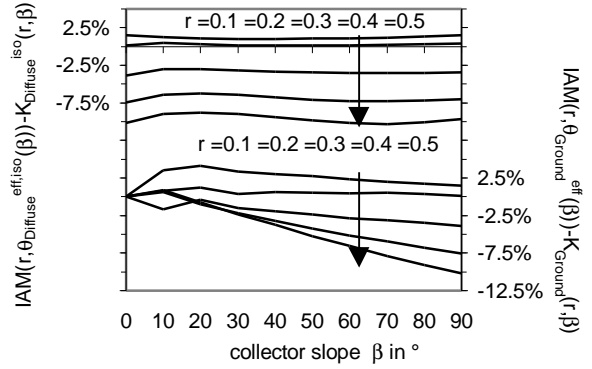
To determine  $\mathbf{q}_{Ground,eff}$  and  $\mathbf{q}_{Diffuse,eff}^{iso}$  Brandemuehl and Beckmann evaluate the following integral formula, which is derived from (6) and (7) with the assumption that the radiation distribution is isotropic in the region of interest.

$$K_x = \frac{\iint_{R(x)} IAM(\mathbf{q}) \cos \mathbf{q} \sin \mathbf{J} d\mathbf{J} d\mathbf{j}}{\iint_{R(x)} \cos \mathbf{q} \sin \mathbf{J} d\mathbf{J} d\mathbf{j}} \quad (11)$$

(Here, x means the diffuse isotropic fraction, the diffuse ground reflected or the diffuse fraction from the horizon. The integration has to be done over the whole area  $R(x)$ , from where the radiation of the corresponding fraction hits the collector.)



a.)



b.)

**Fig.4 Deviation of  $K_{Ground}$  and  $K_{Diffuse}^{iso}$  calculated with  $\mathbf{q}_{Ground,eff}$  resp.  $\mathbf{q}_{Diffuse,eff}^{iso}$  (variant "Brandemuehl") or by integrating (4) (variant "Integration") with (9) for different values of r. For  $r=0.22$  the two variants coincides, since the IAM-function used by Brandemuehl is comparable to the run of  $IAM(r=0.22, \mathbf{q})$ . For higher r the Brandemuehl variant underestimate the Integration variant. This is caused by the fact, that for  $r>0.22$  the higher  $\mathbf{q}$ -angles are weighted in (11) less than they are weighted for  $r=0.22$  and so the Brandemuehl- $\mathbf{q}_{eff}$ -angles overestimates the correct average  $\mathbf{q}_{eff}$ -angles. For  $r=0.5$ , these errors lead to deviations up to 10%-points in  $K_{Diffuse}^{iso}$  and  $K_{Ground}$ .**

The inverse function of the IAM-function was used to determine  $\mathbf{q}_{Ground,eff}$  and  $\mathbf{q}_{Diffuse,eff}^{iso}$ . The  $\mathbf{q}_{eff}$ -values could be interpreted as an average over the incidence angles weighted by the used IAM-function. However, Brandemuehl and Beckmann considered as  $IAM(\mathbf{q})$  only the transmittance and absorption of the collector glazing  $\mathbf{t}(\mathbf{q})$  using the Fresnel-formula with

$n=1.34..1.562$  and  $KL=0.0125..0.0542$ . The run of  $t(q)$  is comparable with that of (3) with  $r=0.22$ . However, typical parameter values of flat plate collectors in test results are  $r=0.27..0.45$ . Considering both  $t(q)$  and the absorption of the absorber  $a(q)$  (for example by eq.4.11.1 in (Duffie and Beckmann, 1991) will lead to results for  $IAM(q)$  comparable to the run of (3) with  $r=0.3-0.4$ . Because of these facts, the using of  $q_{eff}$ -values calculated by Brandemuehl and Beckmann will lead to systematic errors when using them in conjunction with (3) and  $r=0.27...0.45$  to determine  $K_{Ground}$  and  $K_{Diffuse}^{iso}$ . Due to this, (11) was evaluated in this paper with (3) for each  $r$  to determine the correct values of  $K_{Ground}$  and  $K_{Diffuse}^{iso}$  (Variant "integration"). If needed by  $K_X$ ,  $K_{Diffus}^{Hor}$  was furthermore evaluated, defining the horizon as the region  $0^\circ < \vartheta_{Zenite} < 10^\circ$ .

Fig.4 shows that the variant "Brandemuehl" systematically underestimates the correct values of  $K_{Ground}$  and  $K_{Diffuse}^{iso}$  for higher values of  $r$  with up to 10%-points. Since the variant "Brandemuehl" is typically used in the parameter identification process during collector tests the determined collector test parameter (particularly the Ambrosetti-Parameter  $r$ ) might lead to a systematical error due to the systematical underestimation of  $K_{Ground}$  and  $K_{Diffuse}^{iso}$ , shown above.

With the help of the incidence angle correction factors,  $G_{use}$  can be calculated by (7). Therefore, it is possible now to examine the different diffuse fraction and conversion models only considering the radiation, which passes the glazing and is absorbed by the absorber. Fig.5 shows the results on the basis of daily sums  $H_{use}$  of  $G_{use}$  if using  $G^H$  as input and different combination of diffuse correlation and conversion models. Unless no explicit other parameter value of  $r$  is noted all further presented results are calculated with  $r=0.33$ . The variants "Erbs-Max" and "Erbs-Min" show clearly that the deviations from Erbs/Hay-Davies according to the uncertainty of  $k_d$  could be higher than  $0.5 \text{ kWh/m}^2\text{d}$ .

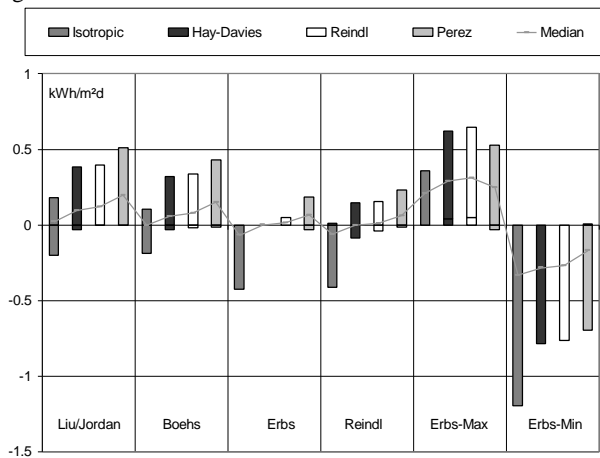


**Fig. 5: Influence of the diffuse correlation and conversion models on the  $H_{use}(G^{H,meas})$ - day sum. Represented in the figure is the median and the 90%-interval of the deviations to the combination Erbs/Hay-Davies, used as a reference.**

#### 4. MEASURING THE GLOBAL RADIATION IN COLLECTOR PLANE

The advantage of measuring the global radiation in the collector plane is the exact knowledge of the radiation sum, which reaches the collector. On the other hand there is the problem of dividing the global radiation into the different direct and diffuse fractions. An upper estimation for  $G_{use}$  is to calculate for each data point:

$$G_{use} = G^T \cdot \text{Max}(K_{Diffuse}^{iso}, K_{Beam}) \quad (12)$$

An lower estimation is analogical:

$$G_{use} = G^T \cdot \text{Min}(K_{Diffuse}^{iso}, K_{Beam}) \quad (13)$$

(Variants "Max( $G^T$ )", "Min( $G^T$ )").

On the other hand there is the possibility to interpret  $G^T = f(G^H)$  in (1) as an implicate function of  $G^H$ , from which  $G^T$  can be evaluated numerically. After this, the division into the different fractions which are needed for calculating  $G_{use}$  can be carried out by the way described in chapter 2. This leads to new uncertainties at high incidence angles, since the implicit function has possibly more than one solution at these angles. Then, the smallest solution of  $G^H$  has been taken.

Fig.6 shows the same values as fig.5 with the difference, that  $H_{use}$  has been calculated with  $G^T$  as input and with the algorithm described above. The comparison with fig. 5 indicates that the uncertainties of  $H_{use}$  due to the different diffuse correlation and conversion models are much lower when using the global radiation, measured in the collector plane. Even in the extreme examples "Erbs-Min" and "Erbs-Max" the deviations do not exceed  $0.1 \text{ kWh/m}^2\text{d}$ . Although Erbs/Hay-Davies seems to be the best approach, fig. 6 indicates that the choice of the correlation/conversion models is of minor importance as long as applying the methods described above. However, the variants "Max( $G^T$ )" and "Min( $G^T$ )" show with uncertainties up to  $0.5 \text{ kWh/m}^2\text{d}$ , that a distribution into the different radiation fractions has to be done.

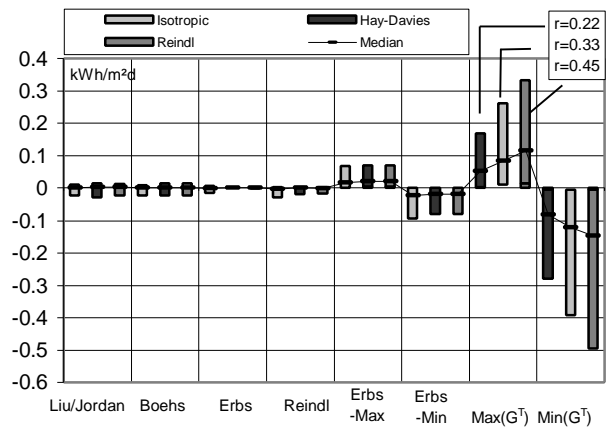


**Fig.6: Influence of the diffuse correlation and conversion models on the  $H_{use}(G^{T,meas})$ - day sum. Represented in the figure is the median and the 90%-interval of the deviations to the combination Erbs/Hay-Davies, used as a reference.**

## 5. VARIANTS OF THE INCIDENCE ANGLE CORRECTIONS

The typical procedure to determine the incidence correction factors  $K_{\text{Ground}}$  and  $K_{\text{Diffuse}}^{\text{iso}}$  is the use of the Brandemuehl- $q_{\text{eff}}$ -values (variant “Brandmuehl”). As described in section 3, this will lead to systematic errors of  $K_{\text{Ground}}$  and  $K_{\text{Diffuse}}^{\text{iso}}$  for  $r \neq 0.22$  of up to 10%-points in comparison to the variant “integration”. Another often used approximation in system simulations is the assumption:  $K_{\text{Diffuse}}^{\text{C}} = K_{\text{Diffuse}}^{\text{Hor}} = K_{\text{Diffuse}}^{\text{iso}}$  i.e., that for considering the IAM-incidence-angle-dependence, the whole diffuse radiation is assumed to be isotropic (Variant “Isotropic IAM”). Which error is implied by these assumptions (variant “Brandmuehl”, variant “isotropic”) on daily sums of  $H_{\text{use}}$ ?

In the background of this question the useful radiation  $G_{\text{use}}$  calculated with the variant “Brandemuehl” and the variant “Isotropic IAM” are compared in fig.7.B-C to  $H_{\text{use}}$  calculated with the more correct “integration variant”. As input for these calculations  $G^{\text{T,meas}}$  was used and the single beam diffuse and ground radiation fractions of  $G^{\text{T}}$  are determined with the algorithm described in chapter 4 in conjunction with the conversion model Erbs/Hay-Davies. Since the deviations depend on the value of the Ambrosetti-Parameter  $r$ , they are shown for three different values. The presented results indicate, that the approximation error of the variant “Brandemuehl” could be significant. The approximation error of the variant “Isotropic IAM” is lower since the continuous approximation errors during the day compensate each other.

Also in fig.7 is shown (cf. A), that  $H_{\text{use}}$  depends strongly on the value of the Ambrosetti-parameter  $r$ . This indicates, that the incidence-angle-modifier-performance may have an important influence on the solar gain of the solar system.

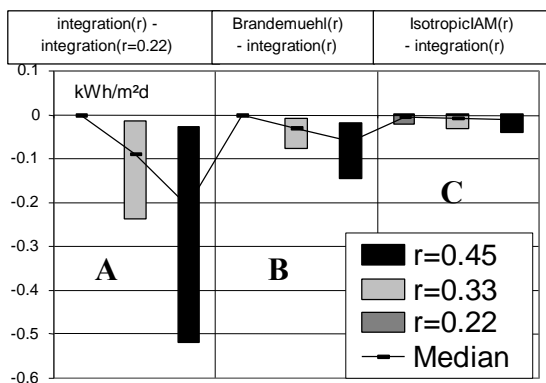


Fig. 7: Deviation of the  $G_{\text{use}}$  daily sum, calculated with the combination Erbs/Hay-Davies from measured global radiation in collector plane for different variants of incidence angle corrections. Represented in the figure is the median and the 90%-interval of the deviations to the variant “integration” used as a reference.

## 6. COMPARISON OF SOLAR SENSORS

The measurement of the global (horizontal) radiation has uncertainties depending on the used solar sensor. To estimate these errors, seven different commercially available solar sensors (cf. tab. 1) have been in operation simultaneously since June 1999 in Marburg (Germany).

Type	Manufacturer	Principle	Investment in Euro
CM 11	Kipp & Zonen	Pyranometer	About 1700
CM 6b	Kipp & Zonen	Pyranometer	About 1125
CM 3	Kipp & Zonen	Pyranometer	About 500
SI-01TC	Mencke & Tegtmeier	PV-Cell	About 175
SPLite	Kipp & Zonen	PV-Cell	About 290
EN 01	TriCom	PV-Cell	About 110
SSR 81	TriCom	PV-Cell	About 230

Tab 1: Solar sensors used in the field test

Fig.8 shows that within the scope of the measured data, which are 1-minute-mean-values, the more accurate PV-cells like SSR 81 and SPLite achieve comparable results to the CM 3 – pyranometer with respect to the mean deviation as well as to the scattering of the single values related to their mean values.

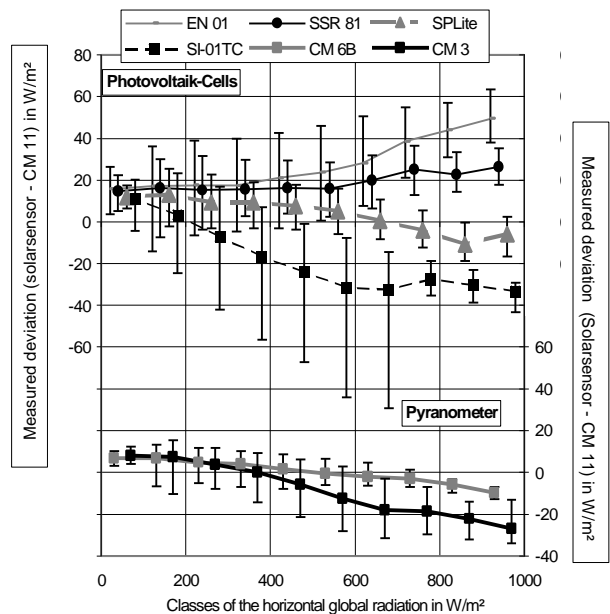


Fig.8: Measured deviation of the different solar sensors from tab.1 to the reference sensor (CM 11). The abscissa describes discret classes of irradiance (width of the classes: 100 W/m², e.g. irradiance in the range of 100-200 W/m²). The plotted values represent the mean values of the deviations for the different classes, the vertical lines represent the sectors, in which 90 % of the deviations are located. (Data basis: 15.7.-30.9.9, 1-min time scale)

The influence of these deviations on the daily sums of the useful radiation  $G_{\text{use}}$  and the solar gain  $Q_{\text{sol}}$  of a solar thermal system is shown in fig.9. For this, the measured values of the reference CM 11 sensor have been transformed corresponding to a linear shift and a superimposed scattering given from fig.8. The annual simulations to determine  $Q_{\text{sol}}$  are made with the system model, that will be presented in the next chapter.

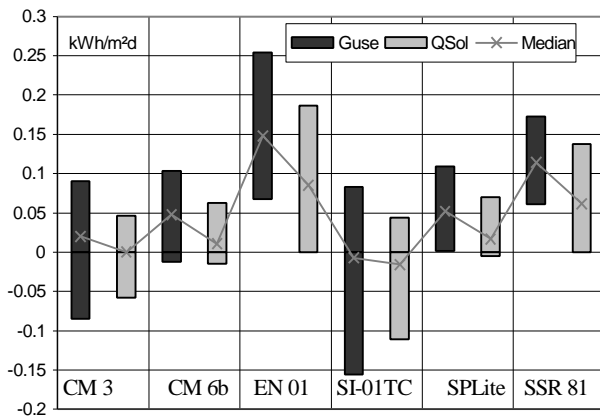


Fig. 9: Influence of the different solar sensors on the daily sum of the useful radiation  $G_{\text{use}}$  and the simulated solar gain  $Q_{\text{sol}}$  of the solar thermal system (described in chapter 7). Represented in the figure is the median and the 90%-interval of the deviations to the results calculated from the CM11-data which are used as a reference. The properly calibrated PV-sensors achieve also in this respect satisfying results compared to the CM3-pyranometer.

We can derive from fig. 9 that the uncertainties of the solar gain if using measured data of a properly calibrated PV-Cell (SPLite) are similar to that with a pyranometer database. With uncertainties in the order of magnitude of lower than 0.1 kWh/m²d it seems to be justifiable (in comparison to the uncertainties derived in section 4) to use a cheaper pyranometer or a calibrated PV-Cell for a monitoring of solar thermal systems.

## 7. SIMULATIONS

The interesting value for the monitoring of solar systems is neither the global radiation in collector plane  $G^T$ , nor the absorbed energy  $G_{\text{use}}$ , but the solar gain  $Q_{\text{sol}}$ . To examine the influence of the different diffuse correlation and conversion models on the estimation of the solar gain of large solar systems, annual simulations of two different existing solar systems (Leipzig, Zwickau) have been carried out. Reasons for the differences of the uncertainties (due to the correlation and conversion models) between the useful radiation and the solar gain of the solar thermal system are:

- The magnitude of the solar gain  $Q_{\text{sol}}$  is only a portion of the useful radiation because of thermal losses to the surroundings,

- uncertainties at low radiation can be neglected,
- uncertainties at very high solar fractions are less important due to high system losses.

Fig.10 shows a system diagram of the solar thermal system installed at a student house in Zwickau (Germany).

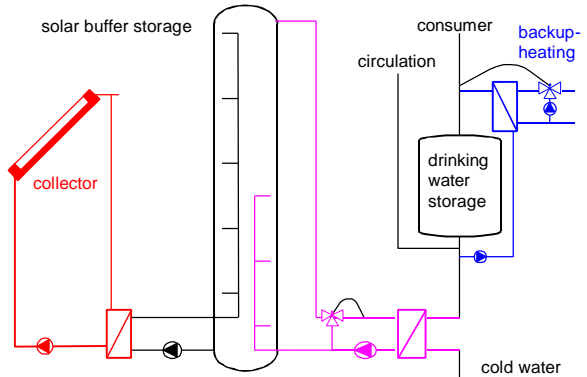


Fig. 10: System diagram of the solar domestic hot water system of two student houses in Leipzig and Zwickau ( $A_{\text{col}}: 157.6 / 398.8 \text{ m}^2$ ,  $V_{\text{storage}}: 9 / 20 \text{ m}^3$ ,  $Q_{\text{load}}/m_{\text{col}}^2\text{day}: 1-11 / 5-20 \text{ kWh/m}^2\text{d}$ ). The systems in Leipzig and Zwickau differ (besides boundary conditions and system and model parameters) slightly in the control strategy for charging and discharging the solar storage.

A detailed system model of the whole system shown in fig.10 was used. The model is built in TRNSYS with standard components and with the UCC-Types MULTIPORT and MFC for modeling storage and collector, respectively. The model parameters are chosen from producer information sheets, test results or are if necessary calculated from measured values. As measurand inputs, the TRNSYS-model uses  $G^T$  or  $G^H$ , the ambient temperature, hot water flow rate and cold water temperature.

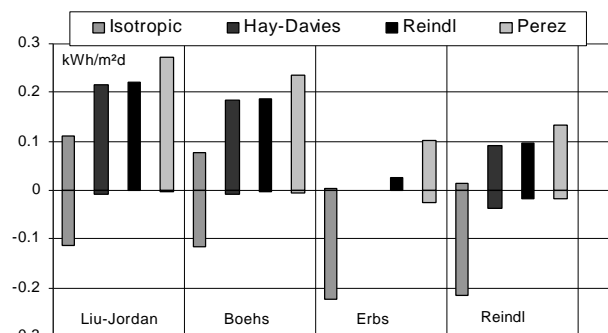
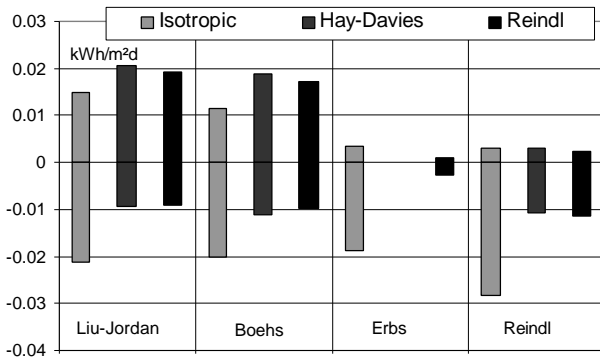


Fig. 11: Influence of the diffuse correlation and conversion methods on the simulated solar gain  $Q_{\text{sol}}$  of a solar thermal system, if the global radiation measured in horizontal plane  $G^H$  is used as input. In the diagram the 90% -interval of the deviations from the correlation Erbs/Hay-Davies are represented. The deviations of the solar gain show the same tendency as corresponding values of the useful radiation (see fig.5), but they are significantly lower.

The simulations yield, as shown in fig.11 and 12, that the uncertainties of the solar gain are systematically the same as the uncertainties of the useful radiation, but with lower absolute

values. It can be derived from the two diagrams, that the uncertainties in the solar gain are in the order of magnitude of 0.2 kWh/m<sup>2</sup>d when measured in horizontal plane and below 0.03 kWh/m<sup>2</sup>d when measured in collector plane. The latter value seemed to be adequate for the monitoring of solar thermal systems.



**Fig. 12: Influence of the diffuse correlation and conversion methods on the simulated solar gain  $Q_{sol}$  of a solar thermal system, if the global radiation measured in collector plane  $G^T$  is used as input. In the diagram the 90% -interval of the deviations from the correlation Erbs/Hay-Davies are represented. The results show, that the deviations are even in the most unfavourable case below 0.03 kWh/m<sup>2</sup>d.**

## 8. CONCLUSION

For monitoring solar thermal systems by the method of comparing calculated and measured solar gains it can be concluded from the results described above:

- The combination of the diffuse fraction estimation from Erbs together with the conversion model from Hay-Davies seems to be the best for the estimation of the diffuse fractions and the following conversion on tilted surfaces. More detailed methods (like Perez or Reindl) do not provide better results.
- The measurement of the global radiation in the collector plane enables an estimation of  $H_{use}$  and  $Q_{sol}$  which reacts less sensitive on the different diffuse-correlation and conversion models than the estimation from the global horizontal radiation. (Variation of  $H_{use} < 0.1$  kWh/m<sup>2</sup>d, Variation of  $Q_{sol} < 0.03$  kWh/m<sup>2</sup>d).
- The Brandemuehl approximation for the incidence angle correction of the non-direct fraction of the radiation can possibly lead to systematic errors of  $H_{use}$  of up to 0.15 kWh/m<sup>2</sup>d.
- The performance of the IAM-correction has an important influence on the simulated solar gain. For this reason IAM-parameters (like the Ambrosetti-parameter) should be chosen with care.

- The deviations between  $H_{use}$  (or  $Q_{sol}$ ) determined from data measured with a properly calibrated PV-sensor, and  $H_{use}$  (or  $Q_{sol}$ ), determined from data measured with the reference sensor (CM 11-pyranometer) are only slightly higher than the uncertainties resulting from the diffuse correlation and conversion models.

## NOMENCLATURE

$A_{coll}$	Collector area, m <sup>2</sup>
F	Reduced brightness coefficients
G	Global irradiance, W/m <sup>2</sup>
H	Daily sum of the global irradiance, kWh/m <sup>2</sup> d
IAM	Incident angle modifier
$I^{ext}$	Extraterrestrial radiation W/m <sup>2</sup>
K	Correction factor
$K_d$	Diffuse fraction
$K_t$	Clearness index
KL	Product of the absorptance of the glass and the width of the glass plate
N	Refraction index
Q	Thermal energy in kWh or daily sum of thermal energy kWh/m <sub>col</sub> <sup>2</sup> d
R	Integration area
r	Ambrosetti parameter
$V_{storage}$	Storage volume, m <sup>3</sup>
x	Different fractions of radiation
<b>a</b>	Absorption
<b>q</b>	Incident angle, °
<b>J, j</b>	incident angles on the collector respective to the two dimension of the (flat plate) collector, °
<b>t</b>	Transmission of radiation through the glass cover
<b>(ta)<sub>⊥</sub></b>	Transmission-absorption product for vertical incidence

### Subscripts:

Beam	Direct fraction
C	Circumsolar fraction
load	Consumption
Diffuse	Diffuse fraction
eff	Effective
Ground	Fraction reflected from the ground
H	Horizontal surface
Hor	Fraction coming from the horizon
Iso	Isotropic fraction
meas	Measured values
sol	Solar gain at the heat exchanger between solar buffer storage and collector
sol2	Solar gain at the solar buffer storage discharging heat exchanger
T	Tilted surface

use Useful, absorbed  
zenith Zenith

## REFERENCES

- (Ambrosetti and Keller, 1985): Ambrosetti, P., Keller, J.: „Das neue Bruttowärmeertragsmodell für verglaste Sonnenkollektoren“, Technischer Bericht des Eidgenössischen Institut für Reaktorforschung (EIR), Würenlingen EIR, 1985
- (Brandemuehl and Beckmann, 1980): Brandemuehl, M. J., Beckmann, W. A.: „Transmission of Diffuse Radiation Through CPC and Flat Plate Collector Glazings“. In: Solar Energy, Vol. 24 (1980), S.511-513
- (Boehs et al. 1976): Boehs, E.C. et al.: „Distribution of Direct and Total Solar Radiation Availabilitites for the U.S.A.“ Sandia Report SAND76-0411, August 1976 cited in TRNSYS – A Transient System Simulation Programm. Manual zu Version 14.1, Madison 1994
- (Duffie and Beckmann, 1991): Duffie, J.A., Beckmann, W.A.: „Solar Engineering of Thermal Processes. 2<sup>nd</sup> ed., New York etc.: John Wiley & Sons. INC., 1991
- (Erbs et al. 1982): Erbs, D. G., Klein, S.A., Duffie, J. A.: „Estimation of the Diffuse Radiation Fraction for Hourly, Daily and Monthly-Average Global Radiation“. Solar Energy 28 (1982), P. 293
- (Hay and Davies 1980): Hay, J. E., Davies, J.A.: „Calculation of the Solar Radiation Incident on a Inclined Surface“, Proc. First Canadian Solar Radiation Data Workshop S.59-72, (1980) cited in TRNSYS – A Transient System Simulation Program. Manual Version 14.1, Madison 1994
- (Liu and Jordan, 1960): Liu, B. Y. H., Jordan, R. C.: „The Interrelationship and Characteristic Distribution of Direct, Diffuse and Total Solar Radiation“, Solar Energy 4 (1960), P.1-19
- (Perez et al. 1988): Perez, R., Stewart, R., Seals, R., Guertin, T.: „The Development and Verification of the Perez Diffuse Radiation Model“, Sandia Report SAND88-7030, October 1988 cited in TRNSYS – A Transient System Simulation Programm. Manual Version 14.1, Madison 1994
- (Reindl et al. 1990): Reindl, D.T., Beckmann, W.A., Duffie, J.A.: „Diffuse Fraction Correlations“, Solar Energy 45 (1990), P.1-8
- (Reindl et al. 1990): Reindl, D.T., Beckmann, W.A., Duffie, J.A.: „Evaluation of Hourly Tilted Surface Radiation Models“, Solar Energy 45 (1990), P.1-8
- (Uecker, 2000): Uecker, M.: „Zur Vermessung, Simulation, Langzeitüberwachung und Optimierung größerer solarintegrierter Wärmeversorgungsanlagen“, preliminary title, Marburg, Dissertation, probably May 2000
- (Ineichen et al. 1990) Ineichen, Pierre, Guisan, O., Perez, R., “Ground-reflected Radiation and Albedo”, Solar Energy 44 (1990), P.207-214

This Research has been supported by the Deutsche Forschungsgemeinschaft and the ROM-Umweltstiftung. The authors wish to thank the TU Chemnitz for making available the data measured in the BMWi-program Solarthermie 2000, used in this presentation.

